Technobius, 2026, 6(2), 0102, DOI: https://doi.org/10.54355/tbus/27897338.6.2.2026.0102

Technobius

https://technobius.kz/

e-ISSN 2789-7338

Article

Mechanical responses of Ili saline loess to EICP treatment under variable salinity and freeze-thaw conditions

Kaixin Shi[1,2], Li Ma[1,2,*], Xuejun Liu[3]

[1]College of Civil Engineering and Architecture, Xinjiang University, Urumqi, China
[2]Xinjiang Key Laboratory of Building Structure and Earthquake Resistance, Xinjiang University, Urumqi, China
[3]Xinjiang Institute of Building Science Co., Ltd, Urumqi, China
*Correspondence: mali@xju.edu.cn

Abstract. This study evaluated the effectiveness of the enzyme-induced carbonate precipitation (EICP) method in improving the mechanical properties of saline loess from Northwest China under different salinity and freeze-thaw conditions. Four different Na_2SO_4 concentrations (0.16%−3.16%) were used to simulate varying degrees of salinization in the Ili loess, and consolidation tests, unconfined compressive strength tests, and freeze-thaw cycle tests were conducted on both treated and untreated specimens. The results show that in consolidation tests, the effect of EICP treatment on the compressibility of saline loess is significantly modulated by salinity – under low-salinity conditions (≤1.16%), the compression index C_c decreased by up to 19.8%; however, under high-salinity conditions (≥2.16%), C_c actually increased by approximately 17%, indicating a reversal of the cementation effect. Unconfined compressive strength tests and freeze-thaw cycle tests showed that, under low salinity conditions, EICP can effectively enhance particle cementation, increasing strength by 15%−39% and improving freeze-thaw resistance. Under high salinity conditions, however, particularly after undergoing six freeze-thaw cycles, calcium carbonate cementation significantly deteriorated, and the strength of treated specimens was lower than that of untreated specimens. The failure mode gradually evolved from end shear and single shear planes to distributed cracking as the number of freeze-thaw cycles increased, ultimately progressing to complete disintegration. In summary, EICP holds engineering potential for reinforcing loess under low salinity conditions; however, in coupled saline-alkali and cold regions, its applicability requires optimized design based on salinity and freeze-thaw conditions.

Keywords: EICP, saline loess, compression characteristics, freezing-thaw cycles.

1. Introduction

Before the term loess was formally introduced and adopted within the geological community, this distinctive sediment was referred to as “Löß” or “Löss” by residents of Heidelberg, Germany, and as “Lehm” by inhabitants of Alsace, France. The term loess first appeared in a formal scientific context in 1824, in Section 89 of Volume III of Charakteristik der Felsarten, authored by the renowned mineralogist Professor Leonhard of the University of Heidelberg [1]. Predominantly composed of silt-sized particles, loess is characterized by a loose fabric, high porosity, and well-developed vertical jointing [2].

Loess deposits, formed primarily during the Quaternary Pleistocene [3], accumulated progressively through aeolian processes under alternating glacial-interglacial climatic conditions. They are widely distributed across Eurasia and parts of the Americas, covering approximately one-tenth of the Earth’s terrestrial surface [4], [5]. As a representative structured unsaturated soil, loess exhibits distinctive engineering properties, including collapsibility, underconsolidation, and pronounced sensitivity to dynamic loading [6], [7]. Under external influences such as rainfall infiltration, snowmelt recharge, and anthropogenic disturbances, its metastable structure is prone to degradation and collapse, potentially triggering geohazards including landslides, ground collapse, and foundation

settlement. In recent years, climate warming has intensified the frequency and magnitude of extreme rainfall and snowmelt events. Coupled with increasing disturbances from urbanization and infrastructure development, loess-related hazards (Figure 1) have shown clear trends toward higher frequency, abrupt initiation, and repeated occurrence, posing significant challenges to regional safety and risk management.

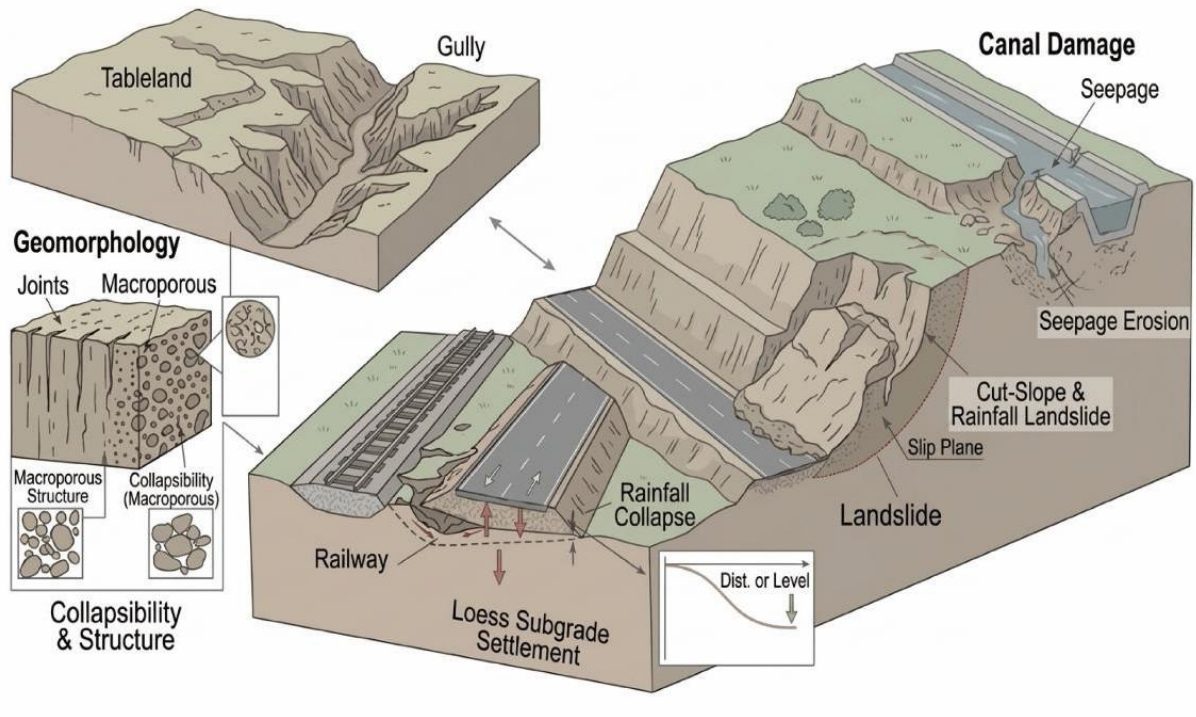


Figure 1 – Typical loess hazards

The Ili Valley in Xinjiang and the Central Asian loess belt are typical sensitive loess regions. In 2017, the Piliqing River landslide evolved into a landslide–damming breach–debris flow disaster chain [8] under the combined effects of prolonged river erosion and freeze-thaw action, while subsequent monitoring showed that the landslide remained in an active deformation state. In 2019, reactivation of a high-position loess landslide in the Zeketai River basin triggered repeated creep movements, forming a ~30 m thick sliding mass that endangers both transportation routes and river safety [9]. Moreover, highway slopes and oil/gas pipelines in Central Asia frequently suffer from shallow slumping and differential settlement under the dual actions of rainfall and collapsibility [10]. The cases presented above reveal that loess disasters are characterized by both marked regional clustering and notable trans-regional commonality. Hence, a systematic investigation of their formation mechanisms and the development of validated prevention-control technologies are of urgent practical importance.

For loess improvement techniques, traditional stabilization methods using cement and lime can enhance strength; however, they are associated with high carbon emissions, significant ecological disturbance, and uncertain long-term durability [11]. In recent years, enzyme-induced carbonate precipitation (EICP), a biochemical coupled ground improvement technique, has attracted increasing attention. This method relies on urease-catalyzed hydrolysis of urea to generate carbonate ions, which subsequently react with calcium ions to precipitate calcium carbonate (Figure 2). The precipitates form microscale cementation bonds between soil particles [12], promoting pore filling and interparticle bridging, thereby reducing the permeability of porous soil media [12], enhancing shear strength, and mitigating collapsibility. Existing studies have demonstrated that EICP can significantly improve the mechanical properties and erosion resistance of sandy soils and some silty soils. Its effectiveness is governed by factors such as solution concentration, enzyme activity, injection strategy, and curing conditions.

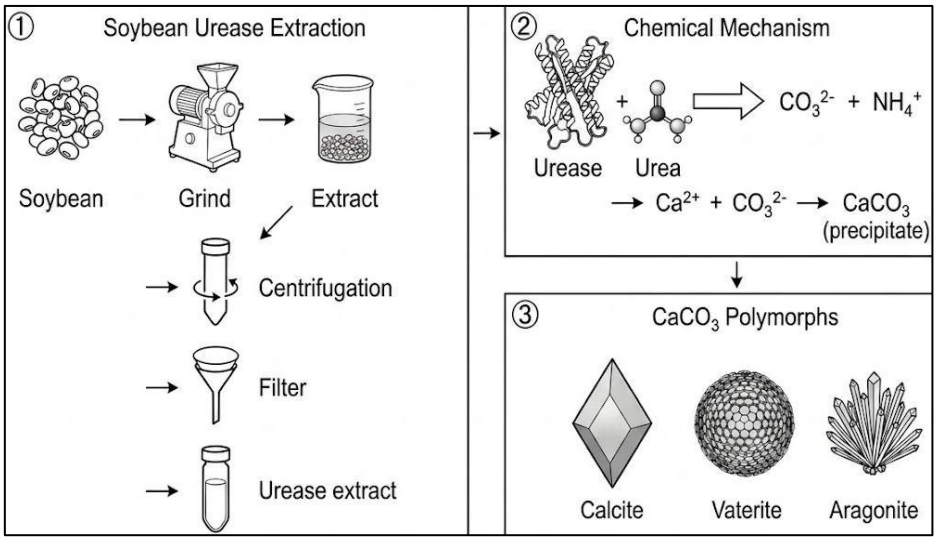


Figure 2 – EICP enzyme extraction procedure and its biomineralization mechanism

However, for the eastern margin of the Central Asian loess belt, particularly the Ili Valley in Xinjiang, where loess genesis is complex, silt content is high, and hydrothermal conditions are distinctive, the mechanisms and engineering applicability of EICP remain insufficiently understood. Specifically: (i) the effects of ion composition and concentration in saline environments on urease activity and calcium carbonate crystallization are not yet well clarified; and (ii) the stability and durability of the cemented soil under coupled multi-physics processes, such as freeze-thaw cycles and wetting-drying cycles, lack systematic evaluation. These limitations constrain the broader application of EICP in loess regions.

Accordingly, this study focuses on loess from the Ili Valley in Xinjiang, investigating the EICP-induced stabilization mechanisms and the mechanical behavior of sulfate-rich saline loess treated with EICP. The findings are expected to provide theoretical support for green bio-mediated improvement of loess and to offer practical guidance for geohazard mitigation and engineering design in northwestern China and other regions with similar geological conditions.

2. Methods

The loess samples used in the experiment were collected from the surface layer (depth of 1−2 m) of a slope in the Hursai loess landslide area of the 61st Regiment, 4th Division, Xinjiang Uygur Autonomous Region, China. The soil is yellowish-brown with sparse fine plant roots. Basic physico-chemical properties were determined following the Chinese standard GB/T 50123-2019 Standard for Geotechnical Testing Method. Mechanical sieving was conducted using standard geotechnical sieves, and laser diffraction analysis was performed using a laser particle size analyzer, Microtrac, USA. The resulting grading curve showed that the grain size distribution spanned a wide range, but the mass was concentrated in the silt fraction 10−100 μm, with low proportions of fine and coarse particles. The gradation exhibits good continuity, yet the dominant particle group (silt) is prominent. The tested loess sample exhibits a specific gravity of 2.7 and a low initial salinity of 0.16%. Its Atterberg limits are characterized by a liquid limit of 27.7% and a plastic limit of 16.5%, resulting in a plasticity index of 11.2, which classifies the soil as a low-plasticity silty clay. The compaction characteristics indicate an optimum moisture content of 16.64% and a maximum dry density of 1.67 g/cm^3.

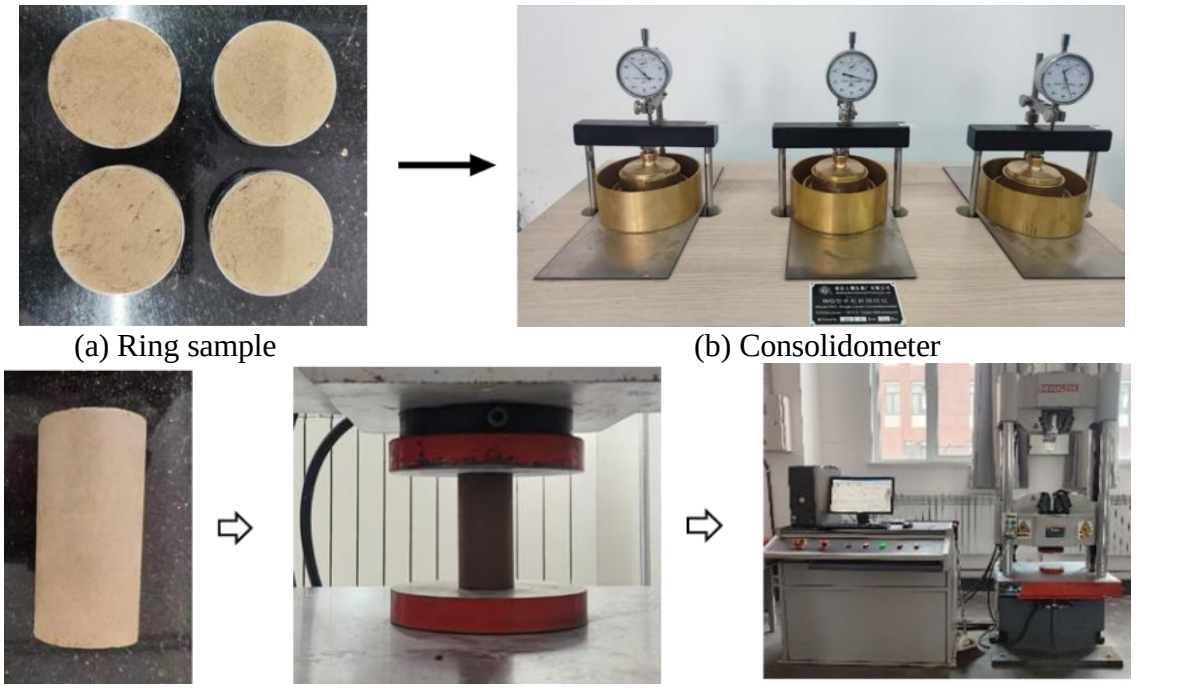
The soil samples were air-dried, pulverized, oven-dried, and sieved through a 2.0-mm mesh before testing. Given the prevalence of chloride-sulfate saline soils in Northwest China, characterized by distinct sulfate transformation behaviors and a dominance of sodium cations, and referencing the standard definition of saline soil (salt content > 0.3%), four specific salinity levels were selected for this study: 0.16% (control), 1.16%, 2.16%, and 3.16%.

First, mix the oven-dried soil evenly with the calculated amount of salt to achieve the target salinity level.

The soybean urease solution is prepared as follows: Mix 20 grams of soybean flour with 1 liter of deionized water and stir for 15 minutes at 25 °C. Then refrigerate the mixture for 24 hours. After refrigeration, filter the suspension through a 500-mesh gauze, then centrifuge at 4,000 rpm for 15 minutes. Collect the resulting supernatant as the soybean urease solution. Determine urease activity using the conductivity method.

To prepare the binding solution, urea and calcium chloride were dissolved in deionized water, with both set at a concentration of 0.5 mol/L. Before sample preparation, the soybean urease solution was mixed with the binding solution at a 2:3 volume ratio to produce the EICP treatment solution.

Subsequently, under continuous stirring, the EICP treatment solution was gradually added to the saline loess until the optimal moisture content of 16.64% was reached, ensuring uniform mixing. The prepared soil samples were then statically compacted into cylindrical specimens with a diameter of 50 mm and a height of 100 mm (Figure 3). After preparation, each specimen was sealed with plastic film and cured at 25 °C for 72 h.



(a) Ring sample (b) Consolidometer

(c) Cylinder sample (d) Loading (e) Universal Testing Machine system

Figure 3 – Specimen preparation and testing setup

Consolidation tests were conducted using a WG-type single-lever consolidometer (Nanjing Soil Instrument Co., Ltd., Nanjing, China) following the standard consolidation test method. Each load increment was maintained until the hourly deformation was less than 0.01 mm before the next load was applied. The loading sequence comprised six vertical pressures: 1, 12.5, 50, 100, 200, and 800 kPa. The tests were performed on both untreated saline loess and EICP-treated saline loess with salt contents of 0.16%, 1.16%, 2.16%, and 3.16%. The target salinity levels were achieved by thoroughly mixing the oven-dried soil with predetermined amounts of analytical-grade sodium sulfate (Na_2SO_4).

Unconfined compressive strength tests were conducted on soil specimens using a universal testing machine with a shear rate of 1 mm/min. The test was terminated when the axial strain continued to increase by 5% after reaching the peak stress. To investigate the freeze-thaw effect on the Ili loess, the freezing temperature was set to −20°C and the thawing temperature to 20°C, with a duration of 12 h for both freezing and thawing, resulting in a 24-h freeze-thaw cycle. The number of freeze-thaw cycles applied to the specimens was 3, 6, and 9, respectively, with 0 cycles serving as the control. After completing the designated freeze-thaw cycles, the specimens were subjected to

unconfined compressive strength tests.

3. Results and Discussion

3.1 Compression tests

From the e-p compression curves of loess with different salt contents in Figure 4, the void ratio of all specimens decreased monotonically as the consolidation pressure increased from 1kPa to 800 kPa. Under the same salt content, the compression curves of the EICP-treated group generally lie above those of the untreated group for most of the loading range, with the most notable difference occurring in the pressure range of 50−200 kPa.

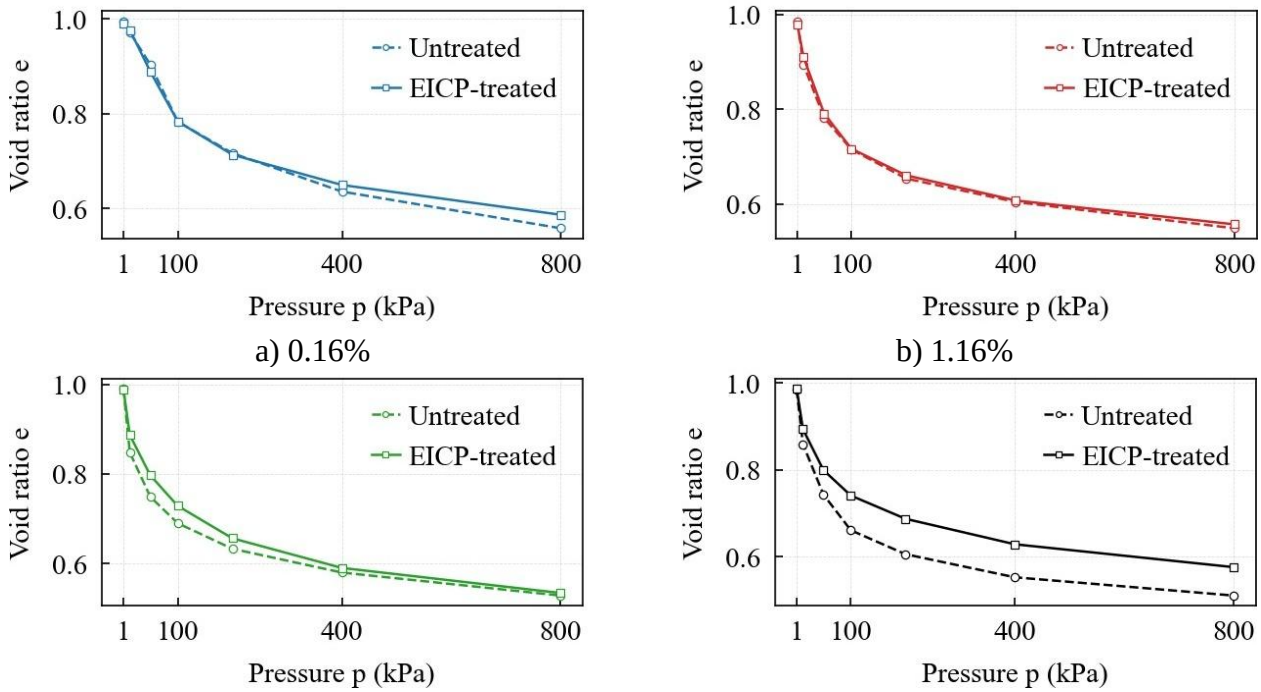


Figure 4 – Compression curves of loess before and after EICP treatment under different salt contents

At the lowest salt content (0.16%), however, the two curves cross near 200 kPa, where the EICP-treated soil shows a slightly lower void ratio than the untreated soil. This observation suggests that the beneficial effect of EICP treatment on compressive deformation resistance may be less pronounced under very low salt conditions, possibly due to insufficient calcium carbonate precipitation or weaker cementation. Nevertheless, for salt contents of 1.16% and above, the EICP-treated curves remain consistently above the untreated curves over the entire pressure range, indicating effective improvement. Regarding the effect of salt content, for untreated loess, the compression curves shift progressively downward as the salt content increases, implying a salt-induced reduction in compressibility. For EICP-treated loess, the trend is not strictly monotonic: the void ratio decreases from 0.16% to 1.16% but increases again at 2.16% and 3.16%. This behavior may result from the dual role of salt, which moderately enhances cementation at low concentrations while potentially inhibiting urease activity or altering crystal morphology at higher concentrations. Previous SEM and XRD analyses of EICP-treated saline soils have shown that $CaCO_3$ precipitates are dominated by vaterite, with minor calcite, and that high-salinity, ion-rich environments can distort vaterite morphology from well-defined spherical forms to disc-like or flake-like crystals. Such morphological distortion reduces the effectiveness of pore filling and interparticle cementation, thereby contributing to strength loss [13].

All compressibility parameters were determined in accordance with the relevant standards.

Specifically, the pre-consolidation pressure (P_c) was computed using a cubic spline curvature maximization technique, which numerically replicates the graphical Casagrande procedure. The remaining parameters were then calculated from Eqs. (1-3), as specified in standards [14] and [15].

$$a_{1-2} = \frac{e_{100} - e_{200}}{200 - 100}, \quad (1)$$

$$E_s = \frac{1 + e_{100}}{a_{1-2}}, \quad (2)$$

$$C_c = \frac{e_{200} - e_{800}}{log_{10}(800) - log_{10}(200)}, \quad (3)$$

where: $a_{1\text{-}2}$ is a coefficient of compressibility; e_{100}, e_{200}, e_{800} are void ratios at 100 kPa, 200 kPa and 800kPa obtained by linear interpolation, respectively; E_s – constrained modulus of deformation (oedometer modulus); C_c – compression index.

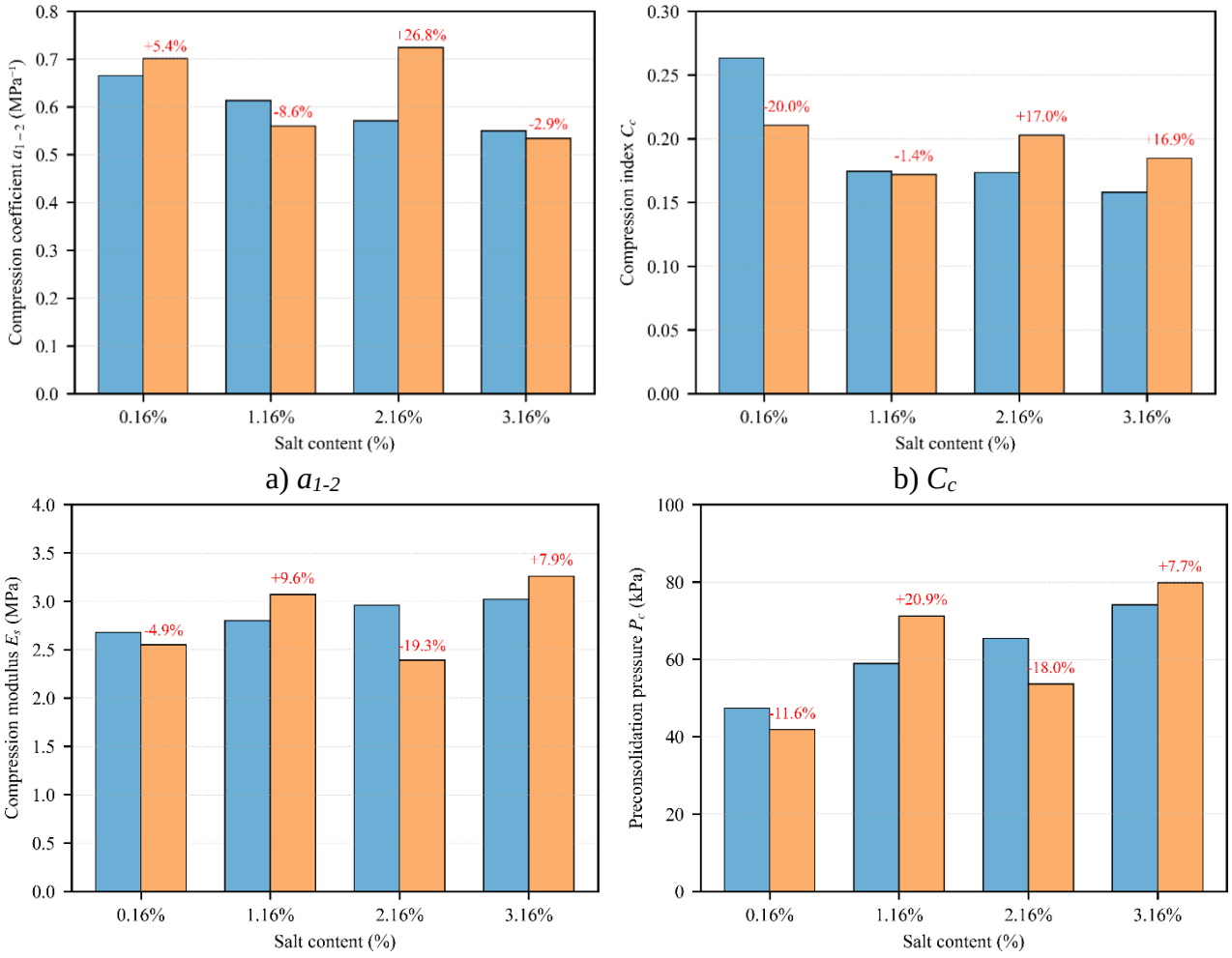


Figure 5 – Compression parameters of untreated and EICP-treated saline loess

Figure 5(a) shows the variation of the compressibility coefficient $a_{1\text{-}2}$ (100-200 kPa) with salt content. For untreated loess, $a_{1\text{-}2}$ decreases gradually from 0.665 MPa^{-1} at 0.16% salt to 0.550 MPa^{-1} at 3.16% salt, indicating that higher salt loading reduces low- to medium-pressure compressibility. After EICP treatment, the effect becomes non-monotonic: at 0.16% salt, $a_{1\text{-}2}$ increases slightly from 0.665 to 0.701 MPa^{-1} (+5.4%); at 1.16% salt, it decreases from 0.613 to 0.560 MPa^{-1} (−8.6%); at 2.16% salt, it increases again from 0.571 to 0.724 MPa^{-1} (+26.8%); and at 3.16% salt, it decreases from 0.550 to 0.534 MPa^{-1} (−2.9%). This inconsistent behavior suggests that the effectiveness of EICP treatment in the 100-200 kPa range is highly sensitive to salt concentration, possibly due to interactions between calcite precipitation and pre-existing salt crystals. Figure 5(b) presents the compression index C_c obtained from the 200-800 kPa normal consolidation range. For untreated

loess, C_c decreases steadily from 0.263 to 0.158 (−40%) as salt content increases, confirming that salt also reduces high-pressure compressibility. EICP treatment produces a clearer pattern: at 0.16% salt, C_c drops from 0.263 to 0.211 (−19.8%); at 1.16% salt the change is negligible (0.174 to 0.172, −1.1%); but at 2.16% and 3.16% salt, C_c unexpectedly increases compared to untreated samples (from 0.173 to 0.203, +17.3%; and from 0.158 to 0.185, +17.1%, respectively). This contrasting trend indicates that EICP-induced cementation effectively reduces compressibility under low-salt conditions, yet becomes detrimental at high salt contents, presumably because the cementation solution disturbs the existing salt-cemented fabric or forms a weaker particle network.

Comparing the two indices, the response of compression parameters at different pressure ranges to EICP treatment differs markedly. In untreated samples, both indices decrease with increasing salt content, showing consistency. However, after EICP treatment, $a_{1\text{-}2}$ displays large non-monotonic fluctuations (e.g., a +26.8% change at 2.16% salt), while C_c shows a more systematic trend: beneficial at low salinity and detrimental at high salinity (2.16% salt). The discrepancy may be attributed to the different pressure ranges: $a_{1\text{-}2}$ reflects the soil's response in the transitional stress stage that may still be influenced by the pre-consolidation pressure, whereas C_c captures the intrinsic compressibility in the fully normal-consolidated region. Therefore, compared with $a_{1\text{-}2}$, C_c provides a more consistent measure for evaluating the long-term effect of EICP treatment on soil compressibility in the normally consolidated stress range (200−800 kPa). The C_c trend clearly reveals that EICP treatment is beneficial only for low-salt loess in this stress regime, but may inadvertently increase compressibility when the salt content reaches approximately 2.16%.

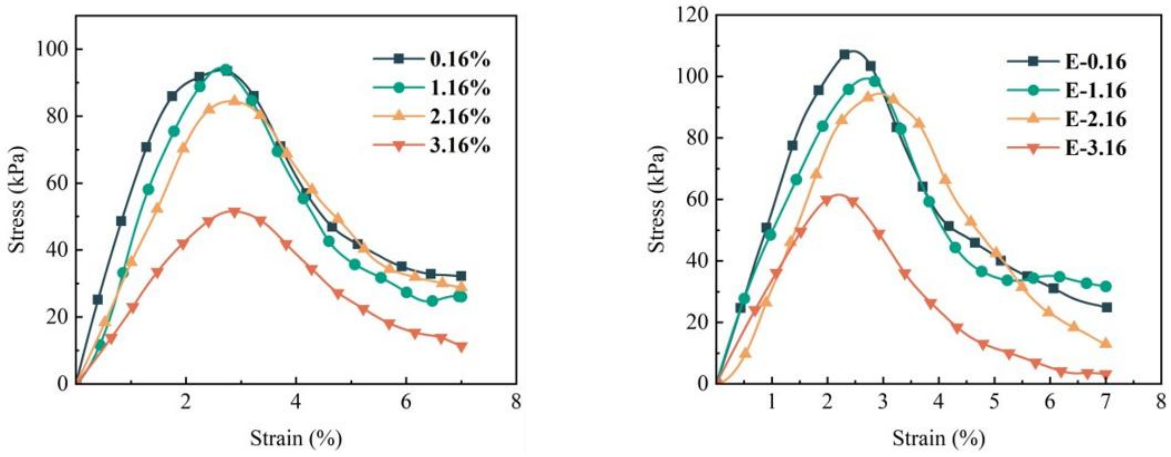
According to the results presented in Figures 5(c) and 5(d), the constrained modulus E_s and the pre-consolidation pressure P_c exhibit broadly similar evolution trends, although the governing physical mechanisms differ to some extent. For the untreated loess, both parameters increase with increasing salt content. Specifically, E_s rises from 2.68 MPa to 3.02 MPa, while P_c increases from 47.3 kPa to 74.1 kPa. This behavior can be attributed to salt-induced crystallization and apparent cementation effects, which enhance interparticle bonding, increase soil stiffness and structural yield strength, and consequently reduce compressibility. For the EICP-treated loess, the response is non-monotonic with respect to salinity. At a low salt content of 0.16%, both E_s and P_c decrease slightly (by 4.9% and 11.6%, respectively), which may be associated with dilution effects of the treatment solution and/or disturbance of the original soil fabric. At salt contents of 1.16% and 3.16%, both parameters increase significantly (E_s: +9.6% and +7.9%; P_c: +20.9% and +7.7%), indicating that a favorable saline environment facilitates calcium carbonate precipitation, thereby promoting effective cementation and enhancing soil stiffness and structural strength. In contrast, at salt content of 2.16%, both parameters decrease markedly (E_s: −19.3%, P_c: −18.0%), suggesting the presence of an unfavorable salinity range in which EICP treatment may disrupt pre-existing salt-crystal skeletons or lead to the formation of weak and discontinuous cementation products.

Overall, E_s and P_c exhibit consistent responses to EICP treatment. Unlike C_c, which captures the high-stress normally consolidated behavior, these two parameters reflect the soil response at low to moderate stress levels. The results indicate that, under these stress conditions, EICP treatment is unfavorable at the lowest salinity (0.16%), beneficial at moderate and high salinities (1.16% and 3.16%), and detrimental at intermediate-high salinity (2.16%). This divergence from the C_c trend underscores that the effect of EICP on saline loess is stress-range-dependent. In practical applications, soils with salt contents of ~2.16% should be avoided, or the treatment formulation should be optimized to accommodate such conditions.

3.2 UCS tests in ambient temperature

Based on the overall trends in the stress-strain curves, the unconfined compressive strength curves of loess under both untreated and EICP-cured conditions, regardless of salt content, exhibit relatively typical phased characteristics and can be broadly divided into a linear elastic stage, a softening stage, and a residual strength stage. In the linear elastic stage (Figure 6a), stress increases approximately linearly with strain; this stage primarily reflects the soil's compression process.

Following the elastic stage, the specimen reaches a peak and enters the softening stage, during which stress begins to decrease, accompanied by the expansion and penetration of internal cracks within the specimen. Subsequently, the specimen enters the residual strength stage. At this point, the main cracks have largely formed, the stress decline becomes more gradual, and the specimen maintains a certain load-bearing capacity primarily through intergranular friction. In terms of failure mode, the untreated specimen exhibited ductile failure characteristics in the soil's compression process, whereas the low-salinity EICP-treated specimen displayed brittle failure. As the salt content increases, EICP-stabilized soil (Figure 6b) exhibits a gradual transition from brittle to ductile behavior. For stabilized specimens with 0.16% and 1.16% salt content, the initial segment of the curve is relatively steep, indicating high soil stiffness; the curve reaches its peak when the axial strain approaches 3% and drops rapidly thereafter. For the solidified specimens with a salt content of 2.16%, the peak stress-strain curve shifted to the rightward, with a slight decrease in peak stress and an increase in ductility. As the salt content rose to 3.16%, the stress-strain curve became flatter; the peak stress decreased by nearly half compared to the 0.16% group and remained at a lower level after reaching the peak.



a) Untreated b) EICP-treated

Figure 6 – Stress and strain curves of saline loess

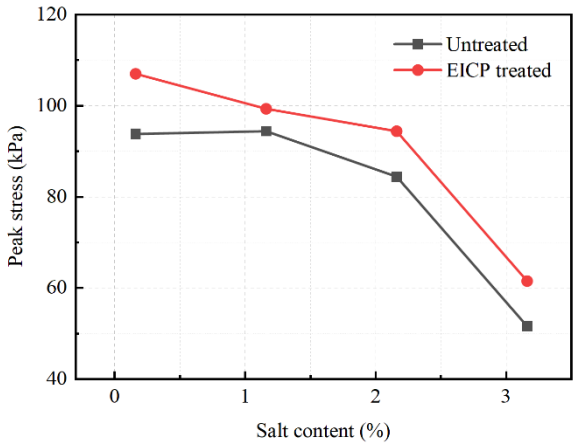


Figure 7 – Peak strength of UCS for saline loess

As shown in Figure 7, salt content has a significant effect on the mechanical properties of untreated specimens. As salt content increases, the peak compressive strength exhibits a monotonically decreasing trend: when the salt content is 3.16%, the specimen strength decreases by approximately 45% compared to the 0.16% group. The primary reason is that aggregates and crystals formed by excess sulfates increase the soil’s porosity and surface roughness, thereby weakening the cementation between particles. In contrast, the EICP-stabilized group exhibited increased strength at all salt content levels, indicating that calcium carbonate cementation played an effective role.

However, the influence of salt content on the reinforcement effect remains quite significant. Specifically, at a salt content of 0.16%, the peak stress reached 108 kPa, approximately 1.15 times that of the untreated group; whereas at a salt content of 3.16%, the peak stress was only 61 kPa, with a significantly reduced increase. When the salt content exceeded 2.16%, the decline in cementation effectiveness accelerated, and its strength characteristics gradually approached those of the untreated soil samples, indicating that high-salt environments inhibit urease activity.

Overall, the EICP technique demonstrated significant reinforcement effects in loess with salt contents of 0.16% and 1.16%; however, when the salt content reached 2.16% or higher, the reinforcement effect was significantly suppressed. Therefore, when applying the EICP technique in high-salinity regions such as the Ili Valley, the inhibitory effect of salt on urease activity must be carefully considered in the mix design.

3.3 Unconfined compressive strength tests following freeze-thaw cycles

Under unconfined compression, soils typically exhibit several characteristic failure modes, including end shearing, barreling, single shear plane, and disintegration. Figure 8 presents the failure patterns of loess specimens subjected to freeze-thaw cycling under unconfined compressive conditions. The results indicate that, with increasing numbers of freeze-thaw cycles, the failure mode progressively evolves from end-dominated shear and distinct single shear planes to distributed cracking, and ultimately to disintegration.

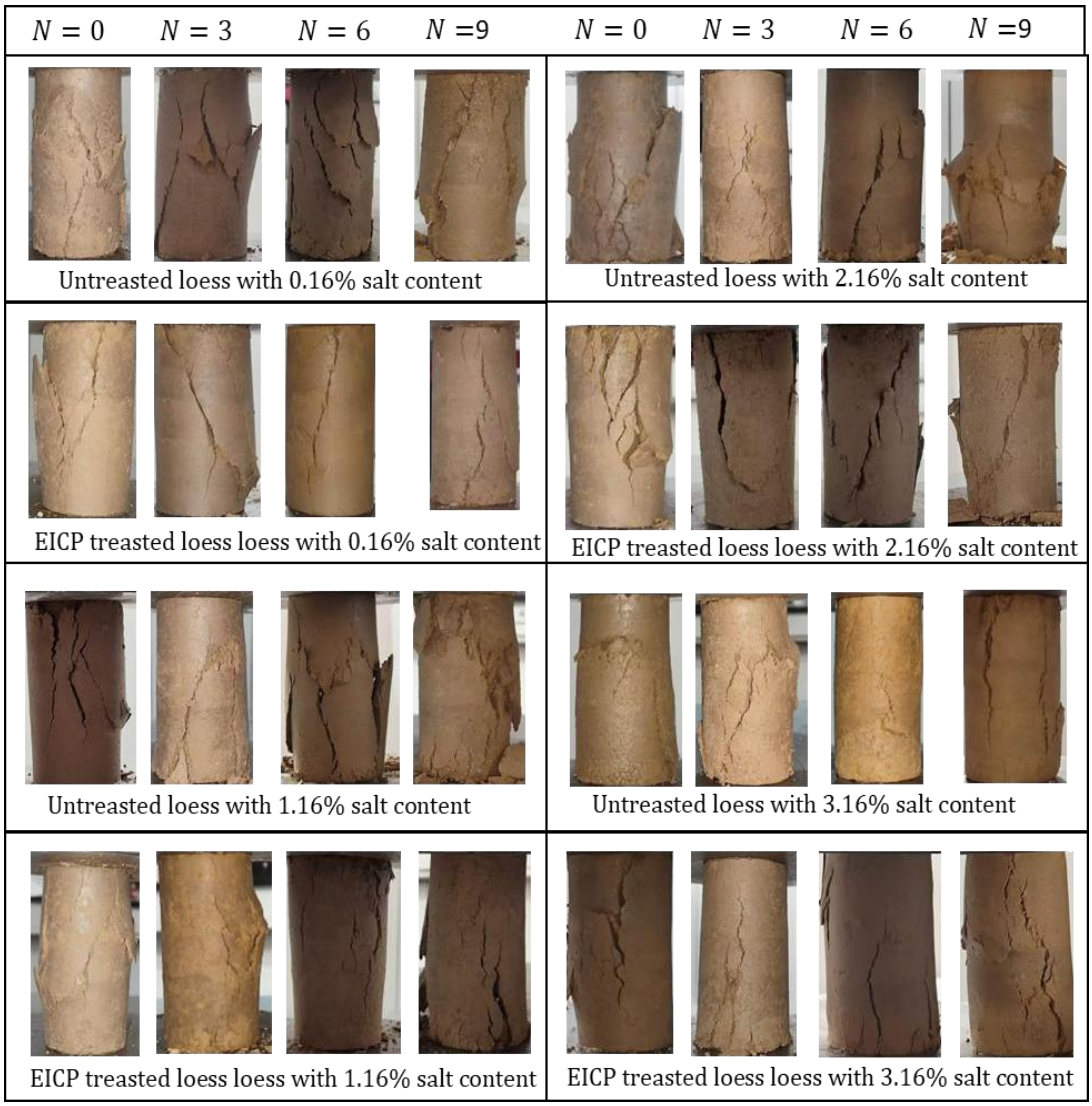
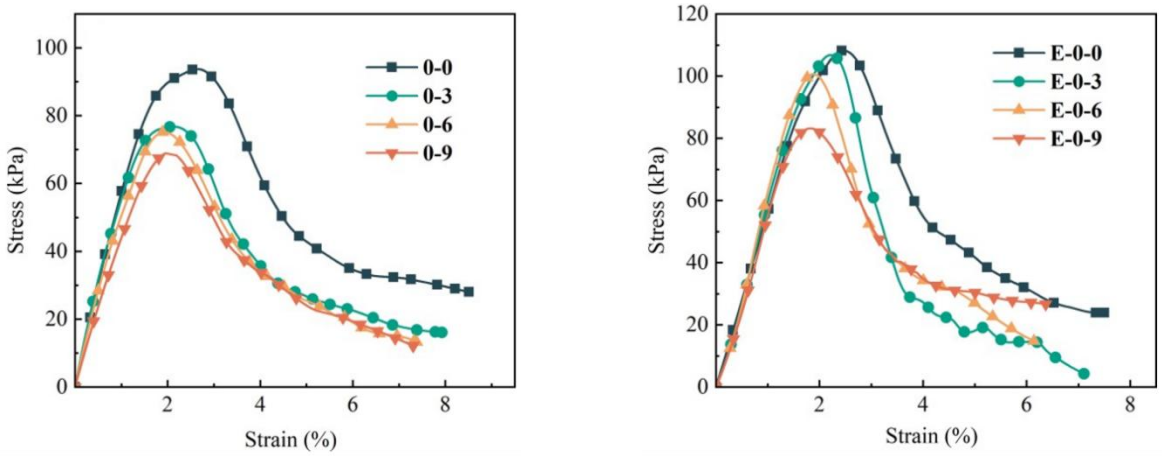


Figure 8 – Failure modes of molded loess specimens after freeze-thaw cycling under UCS testing

An increase in salinity further accelerates this transition by weakening interparticle bonding and inducing crystallization-related damage. Under the combined effects of numerous freeze-thaw cycles and elevated salinity, the specimens exhibit pronounced structural collapse and fragmentation, reflecting a shift from shear-controlled failure to degradation governed by structural deterioration.



a) Untreated b) EICP-treated

Figure 9 – UCS Curves of specimens under 0.16% salinity condition with freeze-thaw cycling

Figure 9 shows the stress-strain curves of untreated and EICP-treated specimens after different numbers of freeze-thaw cycles at a salt content of 0.16%. All specimens exhibited typical stress-strain behavior: a linear elastic stage, a post-peak softening stage, and a residual stage. As the number of freeze-thaw cycles increased, both peak stress and residual strength decreased, indicating that freeze-thaw cycles disrupted internal cohesion within the soil and weakened structural integrity. The strength degradation of the untreated specimens was faster and more pronounced. Although the peak stress of the EICP-treated specimens was higher than that of the untreated group, their ductility decreased with increasing freeze-thaw cycles, indicating that freeze-thaw cycles had a more significant impact on the ductility of the EICP-treated specimens.

The unconfined compressive strength (UCS) of loess is affected by both freeze-thaw cycles and salt content, with higher cycle counts and salinity generally leading to strength reduction. As shown in Figure 10, the bio-cementation formed by EICP treatment significantly enhances the UCS of the specimens, with increases ranging from 15.2% to 39.1% under different freeze-thaw cycles. This demonstrates the effectiveness of EICP in enhancing the freeze-thaw resistance of the soil. Although UCS generally decreases with increasing freeze-thaw cycles, the EICP-treated group exhibits better durability. Taking the salt content of 0.16% as an example (Figure 10(a)), the strength of the untreated specimen decreases by approximately 18% after three freeze-thaw cycles, while the EICP-treated specimen loses only 23% of its strength after nine cycles, indicating a substantially slower rate of deterioration per cycle.

Across all panels of Figure 10, a higher salt content leads to a significant decrease in the peak strength of untreated specimens, with the peak stress decreasing from 94.4 kPa at a salt content of 0.16% to 63.4 kPa at 3.16%, a reduction of 32.8%. Focusing on the 1.16% salt group (Figure 10(b)), after EICP treatment, the specimens maintain a relatively high peak stress and good strength retention; however, the slope of the post-peak softening stage becomes steeper compared with the untreated specimens, indicating reduced ductility. Regarding the freeze-thaw effect, EICP treatment significantly improves the freeze-thaw resistance of the specimens. At a salt content of 1.16%, the strength of untreated specimens decreases by approximately 22.5% after three freeze-thaw cycles, showing pronounced deterioration. In contrast, the strength of EICP-treated specimens decreases by only about 21.4% after nine freeze-thaw cycles, demonstrating that EICP treatment effectively retards strength reduction and enhances structural stability.

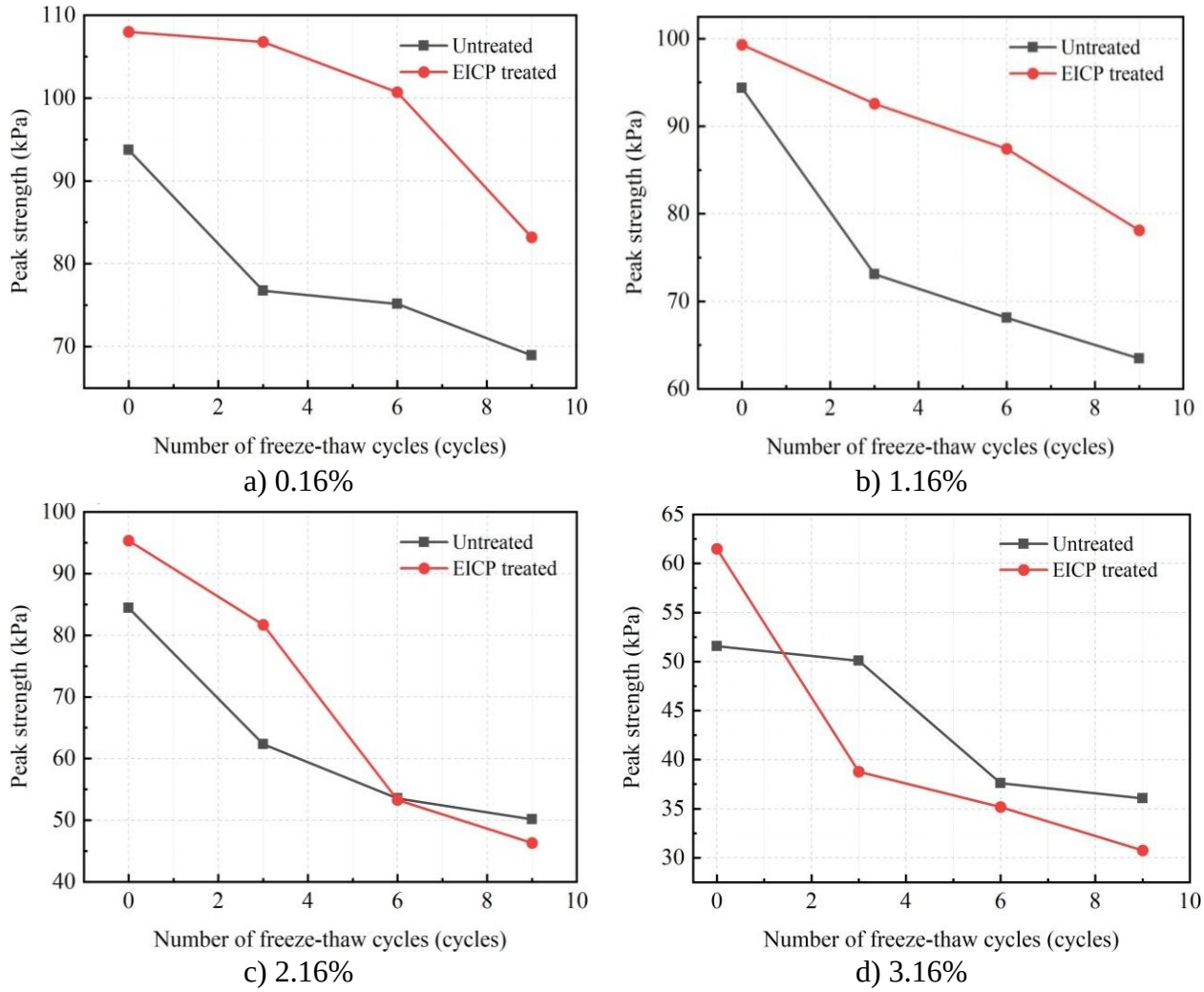


Figure 10 – Peak strength of saline loess with various salt content following freeze-thaw cycles

Figure 10(c) presents the variation in peak unconfined compressive strength (UCS) of specimens with a salt content of 2.16% before and after EICP treatment under different numbers of freeze-thaw cycles. Compared with the specimens at salt contents of 0.16% and 1.16%, the stress-strain curves of the 2.16% salt content specimens also exhibit the three characteristic stages of elastic loading, post-peak softening, and residual response. However, the reduction in peak strength is significantly greater, indicating that a high-salt environment has a more pronounced deterioration effect on the soil structure. As the number of freeze-thaw cycles increases, the strength of the EICP-treated specimens gradually decreases from 95.4 kPa to 46.3 kPa. Notably, after six freeze-thaw cycles, the strength of the EICP-treated specimens becomes lower than that of the untreated loess. Despite the continuous decline in peak strength with increasing freeze-thaw cycles, the peak strain of the EICP-treated specimens remained consistently higher than that of the untreated specimens across all cycle levels. Under 0, 3, 6, and 9 freeze-thaw cycles, the peak strains of the EICP-treated loess were approximately 3.0%, 5.0%, 5.5%, and 5.4%, respectively, whereas those of the untreated loess merely ranged from 2.3% to 2.8%. This observation indicates that, under the high-salt condition of 2.16%, EICP treatment substantially alters the deformation characteristics of the soil, shifting the failure mode from the brittle behavior observed at low salt contents toward a distinctly more ductile failure with enhanced deformability.

Figure 10(d) shows that for specimens with a salt content of 3.16%, the overall trend is generally consistent with that of the other salt content groups (0.16%, 1.16%, and 2.16%), all exhibiting the characteristic stages of elastic loading, post-peak softening, and residual response. Nevertheless, with increasing salt content, the peak strength decreases significantly, and the post-peak drop becomes steeper, indicating that a high-salt environment markedly weakens the structural

stability and cementation strength of the soil.

As the number of freeze-thaw cycles increases, the strength of the EICP-treated specimens continuously decreases, showing a more pronounced degradation trend compared with the untreated specimens. After only three freeze-thaw cycles, the strength of the EICP-treated specimens falls below that of the untreated loess. This turning point occurs earlier than in the 2.16% salt group, demonstrating that the freeze-thaw action damages the bio-cemented structure more rapidly under a high-salt environment. This accelerated degradation is consistent with microstructural observations from analogous MICP-treated sulfate saline soils, where SEM-EDS imaging showed that elevated Na_2SO_4 contents shifted carbonate precipitation from interparticle contacts and pore spaces toward predominantly particle-surface coating. This transition weakened the contact-bonding network and produced a less integrated fabric, making the treated soil more susceptible to freeze-thaw-induced cracking, spalling, and cementation loss [16].

A further comparison of peak strain reveals that, under 0, 3, 6, and 9 freeze-thaw cycles, the peak strains of the EICP-treated loess were approximately 2.2%, 5.2%, 8.2%, and 8.8%, respectively, whereas those of the untreated loess were 2.8%, 4.0%, 6.8%, and 9.8%, respectively. The EICP-treated specimens exhibited a higher peak strain than the untreated specimens at 3 and 6 cycles, but a lower peak strain at 0 and 9 cycles, indicating no consistent benefit in deformability. This result suggests that, at a salt content of 3.16%, freeze-thaw cycling leads to severe structural deterioration in both treated and untreated soils, and both exhibit pronounced flow-plastic deformation characteristics. Under such high-salinity conditions, freeze-thaw damage may progressively weaken the cemented structure, leading to unstable deformation behavior and reduced post-peak stability.

In summary, under the high-salt condition of 3.16%, the strengthening effect of EICP treatment is significantly weakened. Although the EICP-treated specimens may retain limited deformation capacity at certain freeze-thaw stages, this effect is not consistent. With increasing freeze-thaw cycles, the calcium carbonate-cemented structure gradually deteriorates, resulting in rapid strength loss, unstable deformation behavior, and reduced post-peak stability.

It should be noted that the mechanical effect of salinity is loading-mode dependent. Under one-dimensional compression, salt crystallization and pore filling may increase apparent stiffness and structural yield strength, as reflected by the reduced compressibility and increased E_s and P_c of untreated loess. In contrast, under unconfined compression, excessive salinity may weaken effective interparticle bonding and reduce post-peak stability, leading to lower UCS strength and more pronounced softening behavior.

Overall, under salt content conditions of 0.16% and 1.16%, EICP curing can consistently improve the initial strength of the soil and maintain a peak strength higher than that of the untreated group during 0 to 9 freeze-thaw cycles. The rate of strength degradation is relatively gradual, demonstrating good freeze-thaw durability. When the salt content reaches 2.16% or higher, the strength of EICP-treated soil deteriorates more rapidly after initial freeze-thaw cycles, and the peak strength falls below the untreated level after a certain number of cycles. As the salt concentration increases further, this reversal point occurs significantly earlier: it occurs during the 6th cycle for the 2.16% salt group and as early as the 3rd cycle for the 3.16% salt group.

4. Conclusions

1. EICP treatment significantly modified the mechanical behavior of saline loess, and the improvement effect was strongly dependent on salt content. Under low-salt conditions (≤1.16%), the treated specimens exhibited a reduced compression index C_c (by up to 19.8%), indicating suppressed structural collapse and improved resistance to particle rearrangement. However, this beneficial effect was not sustained with increasing salinity. At salt contents ≥2.16%, C_c increased by approximately 17% after treatment, suggesting that excessive salinity adversely affects the development and continuity of interparticle bonding during EICP treatment.

2. Salinity therefore exerts a dual effect on EICP-treated loess. Low salt levels facilitate

calcium carbonate precipitation and enhance stiffness and structural strength, whereas unfavorable salinity conditions, particularly at 2.16%, consistently represent the most unfavorable condition content, weaken the macroscopic improvement effect, and reduce treatment effectiveness. This behavior may be associated with changes in solution chemistry, salt–soil interaction, and the spatial distribution of cementation products; however, the underlying microstructural and chemical mechanisms require further verification. Although previous studies have examined salinity-related changes in $CaCO_3$ polymorphism and crystal morphology in EICP-treated saline soils, as well as the microstructural deterioration of MICP-treated sulfate saline soils under freeze-thaw cycling, direct SEM/XRD evidence for the coupled effects of sulfate salinity, EICP treatment, and freeze-thaw cycling in loess remains limited. This gap motivates the microstructural investigations recommended for future work.

3. Freeze-thaw cycling further accelerates structural degradation, driving a transition in failure mode from end-dominated shear and single shear planes to distributed cracking and eventual disintegration. Under low-salinity conditions, EICP enhanced strength and delayed degradation under cyclic freeze-thaw conditions, with unconfined compressive strength increasing by 15−39%. However, under high salinity conditions, particularly after 6 freeze-thaw cycles, the beneficial effects of EICP diminished or even reversed, with treated specimens exhibiting lower strength than untreated ones. These results indicate that under adverse salinity conditions, the long-term effectiveness of EICP treatment can be severely compromised.

4. These findings suggest that EICP is a promising ground improvement technique for loess soils; however, in saline–alkali and cold regions, its performance depends largely on environmental compatibility and requires targeted optimization, such as adjusting the cementation solution formulation or pre-treating the soil to mitigate salt interference, to ensure reliable field application.to ensure reliable field application.

Acknowledgments

This work was supported by Tianshan Talent Training Program (Grant No. 2023TSYCLJ0055), Xinjiang University “Outstanding Graduate Student Innovation Project” (Grant No. XJDX2025YJS222).

References

[1] H. Ding, Y. Li, Y. Yang, and X. Jia, “Origin and evolution of modern loess science – 1824 to 1964,” *Journal of Asian Earth Sciences*, vol. 170, pp. 45–55, 2019, doi: 10.1016/j.jseaes.2018.10.024.

[2] D. R. Muhs, “Loess Deposits, Origins and Properties,” in *Encyclopedia of Quaternary Science*, Amsterdam, Netherlands: Elsevier, 2007, pp. 1405–1418. doi: 10.1016/B0-44-452747-8/00158-7.

[3] Y. Li, W. Shi, A. Aydin, M. A. Beroya-Eitner, and G. Gao, “Loess genesis and worldwide distribution,” *Earth-Science Reviews*, vol. 201, p. 102947, 2020, doi: 10.1016/j.earscirev.2019.102947.

[4] K. Pye, “The nature, origin and accumulation of loess,” *Quaternary Science Reviews*, vol. 14, no. 7–8, pp. 653–667, 1995, doi: 10.1016/0277-3791(95)00047-X.

[5] Y. Li *et al.*, “Atmospheric dust dynamics over Central Asia: A perspective view from loess deposits,” *Gondwana Research*, vol. 109, pp. 150–165, 2022, doi: 10.1016/j.gr.2022.04.019.

[6] J. M. Plata, J. C. Balasch, J. Boixadera, A. Baltiérrez, F. Preusser, and R. M. Poch, “Source areas and paleoenvironmental reconstruction of the Serra d’Almenara loess (NE Ebro Valley, Iberian Peninsula) from grain-size and heavy mineral signatures,” *Geomorphology*, vol. 451, p. 109085, 2024, doi: 10.1016/j.geomorph.2024.109085.

[7] X. Han, Z. Hu, H. Li, Y. Yin, B. Zhang, and L. Zhang, “Study on the mechanical properties and microstructural evolution of loess under different wet dry and freeze thaw coupled cycling paths,” *Case Studies in Construction Materials*, vol. 21, p. e03924, 2024, doi: 10.1016/j.cscm.2024.e03924.

[8] M. Zhuang *et al.*, “Mechanistic Investigation of Typical Loess Landslide Disasters in Ili Basin, Xinjiang, China,” *Sustainability*, vol. 13, no. 2, p. 635, 2021, doi: 10.3390/su13020635.

[9] Y. Xian, X. Wei, N. Chen, Y. Qi, and H. Xu, “The effects of snowmelt on loess landslides in Tian Shan, China,” *Journal of Hydrology: Regional Studies*, vol. 62, p. 102995, 2025, doi: 10.1016/j.ejrh.2025.102995.

[10] I. J. Smalley *et al.*, “The formation of loess deposits in the Tashkent region and parts of Central Asia; and problems with irrigation, hydrocollapse and soil erosion,” *Quaternary International*, vol. 152–153, pp. 59–69, 2006, doi: 10.1016/j.quaint.2005.12.002.

[11] K. Martin, H. K. Tirkolaei, and E. Kavazanjian, "Enhancing the strength of granular material with a modified enzyme-induced carbonate precipitation (EICP) treatment solution," *Construction and Building Materials*, vol. 271, p. 121529, 2021, doi: 10.1016/j.conbuildmat.2020.121529.
[12] I. Ahenkorah, M. M. Rahman, M. R. Karim, and S. Beecham, "Enzyme induced calcium carbonate precipitation and its engineering application: A systematic review and meta-analysis," *Construction and Building Materials*, vol. 308, p. 125000, 2021, doi: 10.1016/j.conbuildmat.2021.125000.
[13] Z. Zhang, K. Wang, C. Cui, and L. Yu, "Performance and Mechanism of Enzyme-Induced Carbonate Precipitation (EICP) for Fine-Grained Saline Soil Stabilization," *Applied Sciences*, vol. 16, no. 2, p. 1057, 2026, doi: 10.3390/app16021057.
[14] "GB/T 50123-2019 Standard for geotechnical testing method," Beijing, China: China Planning Publishing House, 2019, p. 508.
[15] "ASTM D2435/D2435M-11(2020) Standard Test Methods for One-Dimensional Consolidation Properties of Soils Using Incremental Loading," West Conshohocken, PA: ASTM International, 2020, p. 14.
[16] L. Xiong, L. Tian, X. Zhang, M. Wang, and A. Ahemaiti, "Mechanical properties and microstructural analysis of MICP-reinforced coarse-grained saline soils under freeze-thaw cycling," *PLoS One*, vol. 20, no. 11, p. e0336266, 2025, doi: 10.1371/journal.pone.0336266.

Information about authors:
Kaixin Shi – Master Candidate; 1) College of Civil Engineering and Architecture, Xinjiang University, Urumqi, China; 2) Xinjiang Key Laboratory of Building Structure and Earthquake Resistance, Xinjiang University, Urumqi, China; 107552304720@stu.xju.edu.cn
Li Ma – PhD, Associate Professor, Master Supervisor; 1) College of Civil Engineering and Architecture, Xinjiang University, Urumqi, China; 2) Xinjiang Key Laboratory of Building Structure and Earthquake Resistance, Xinjiang University, Urumqi, China; mali@xju.edu.cn
Xuejun Liu – Professorate Senior Engineer, Xinjiang Institute of Building Science Co., Ltd, Urumqi, China, 625184594@qq.com

Author Contributions:
Kaixin Shi – data collection, testing, modeling, analysis, visualization, interpretation, drafting.
Li Ma – funding acquisition, concept, methodology, resources, editing.
Xuejun Liu – analysis, interpretation.

Conflict of Interest: The authors declare no conflict of interest.

Use of Artificial Intelligence (AI): AI was used to assist in literature screening and language refinement, as well as to aid in the creation of Figures 1 and 2, which were generated with the assistance of an AI image generation tool. All content was critically reviewed, verified, and edited by the authors to ensure accuracy and scientific integrity.

Received: 28.04.2026
Revised: 20.06.2026
Accepted: 22.06.2026
Published: 24.06.2026

Copyright: © 2026 by the authors. Licensee Technobius, LLP, Astana, Republic of Kazakhstan. This article is an open access article distributed under the terms and conditions of the Creative Commons Attribution (CC BY-NC 4.0) license (https://creativecommons.org/licenses/by-nc/4.0/).